



Design Project report

*Assessing the influence of cultivated tropical soils
on natural regeneration*

Students :

Camille Perrin
Alena Vasilyeva

Supervisor arboRise :

Philippe Nicod

Supervisor EPFL :

Meret Aeppli

EPFL

June 5, 2026

Spring 2026

Contents

1	Introduction	2
1.1	Background	2
1.2	Literature review	2
2	Objectives	3
2.1	Expectations	3
2.1.1	Particle size distribution	3
2.1.2	Moisture content	3
2.1.3	pH	3
2.1.4	Soil organic carbon	3
2.1.5	Phosphorus	4
2.1.6	Macronutrients	4
2.1.7	Trace metals	4
3	Methods	4
3.1	Presenting the samples	4
3.2	Sample collection	6
3.3	Sample laboratory analysis	7
3.3.1	Stone content and soil color	7
3.3.2	Particle size distribution	7
3.3.3	Moisture Content	7
3.3.4	pH	7
3.3.5	Soil Organic Carbon	8
3.3.6	Macronutrients and trace metals	8
3.4	Multivariate analysis	8
4	Results	8
4.1	Stone content and soil color	8
4.2	Particle size distribution	9
4.3	Moisture content	11
4.4	pH	12
4.5	Soil organic carbon	12
4.6	Macronutrients and Trace metals	14
4.7	Multivariate Analysis	17
5	Discussion	19
5.1	Recommendations	21
5.2	Limitations	22
5.3	Conclusion	22

1 Introduction

1.1 Background

Climate change represents one of the most pressing challenges of our time, driving rising global temperatures and accelerating biodiversity loss. Among the most promising mitigation strategies, reforestation stands out for its dual role: trees act as carbon sinks by absorbing CO₂ through photosynthesis and storing it in their biomass, while simultaneously providing habitat for countless plant and animal species. Forests also deliver a wide range of essential ecosystem services, from biodiversity conservation and wood production to local climate regulation [1].

Within this global challenge, sub-Saharan Africa is particularly vulnerable. Its dependence on agriculture, the economic sector most exposed to climatic shifts [2], makes the consequences of environmental degradation strongly noticeable. Climate projections suggest more intense droughts, longer dry seasons, and increasingly inconsistent rainfall patterns. In addition, the depletion of soil nutrients occurs as a consequence of soil erosion, but also as a result of certain management practices, such as slash-and-burn cultivation and other subsistence farming practices that do not allow for the replenishment of the nutrients removed from the soil by crops [3]. Slash-and-burn practices are common in Guinea. This combination of factors lead to damaged soils in this region. In this context, reforestation offers a concrete pathway to restoring agricultural conditions by improving soil fertility and water retention [4], supporting the family farming systems that form the backbone of food security across the region [5].

It is in this context that ArboRise, a non-profit foundation dedicated to restoring natural ecosystems, is implementing reforestation campaigns across Guinea with the aim of establishing a wildlife corridor linking the natural parks of these countries through agroforests [6]. The initial focus area spans the sub-prefectures of Linko, Damaro, and Konsankoro in the Prefecture of Kérouané, Republic of Guinea, situated in a climatic transition zone between the humid tropical south and the arid Sahelian north. This region is projected to experience accelerated warming (+1.5°C), increased precipitation volume (+5%), and a more severe dry season, with 30 additional extremely hot days per year by 2030 under the RCP 6.0 scenario [7]. The soils of this area are typically of highly weathered tropical environments: low in natural fertility, limited in organic matter, and frequently deficient in phosphorus, which is one of the primary limiting nutrients for plant growth across sub-Saharan Africa [5].

Over 840 parcels across 26 villages have been sown since 2021 through direct seeding with a mixture of forty native tree species selected for their non-wood forest products and ecosystem services. Early monitoring campaigns have revealed strong heterogeneity in tree growth between, and frequently within parcels. Understanding what drives this variability is essential to guide sustainable land management and optimize reforestation outcomes in degraded environments. The soil's capacity to support tree growth will therefore be assessed through a range of physical and chemical analyses. Physical characterization will include particle size distribution and moisture content, while chemical analyses will cover pH, organic carbon content and macro- and micronutrient availability.

1.2 Literature review

The literature highlights that tropical soils, particularly in West Africa, are characterized by advanced weathering, low natural fertility, and high susceptibility to degradation [8]. Under humid tropical conditions, intense rainfall promotes the leaching of base cations such as calcium, magnesium, and potassium, progressively replacing them with hydrogen and aluminum ions and driving soil acidification [9]. Phosphorus is frequently identified as a primary limiting nutrient in these environments, as its bioavailability is strongly controlled by soil pH: under acidic conditions, iron and aluminum oxides adsorb phosphate ions, forming stable complexes that render phosphorus largely unavailable for plant uptake [10, 11]. Soil texture further modulates fertil-

ity through its influence on cation exchange capacity and water retention, with finer-textured soils generally providing greater nutrient-holding capacity [12]. Slash-and-burn agriculture, the dominant land management practice in the study region, exacerbates these natural constraints by removing base cation reserves through burning and accelerating erosion during the cropping phase, while shortened fallow periods prevent adequate soil recovery [13, 14]. Natural regeneration in degraded tropical environments is governed by a combination of soil chemical properties, seed availability, and microclimatic conditions, with pH, phosphorus availability, and base cation status playing a central role in determining which species can establish and thrive [15]. Together, these findings from the literature guided the selection of soil parameters analysed in this study.

2 Objectives

The main hypothesis of this project is that variations in soil properties across formerly cultivated tropical sites are correlated with natural regeneration and the growth of trees established through direct seeding. It aims to identify the key pedological factors explaining differences in tree establishment and growth between sites. More specifically, the project will compare soil characteristics between high-performing and low-performing parcels at different stages of regeneration, with the goal of developing indicators for the early identification of low growth potential. Finally, suitable soil amendment strategies will be identified by integrating the results obtained in this study with evidence and recommendations from the scientific literature. The recommendations should be concrete and applicable within the Guinean context. The proposed solutions must be technically realistic and economically accessible to the farming families involved in the program. The objective is to enhance the effectiveness of future reforestation campaigns.

2.1 Expectations

2.1.1 Particle size distribution

The determination of particle size distribution, including sand, silt, and clay fractions, is essential for understanding soil texture. Soil texture influences water retention, drainage, aeration, and root penetration, all of which are critical factors for tree development [16]. We expect our analyses to reveal a balanced proportion of sand, silt, and clay for the more productive soils as the most favorable soils for tree growth are loamy soils, ensuring both good drainage and adequate water and nutrient retention.

2.1.2 Moisture content

Soil moisture content is a key physical parameter, as it indicates the amount of water available in the soil for plant uptake. It directly affects nutrient transport, microbial activity, and root function. Both excessive and insufficient moisture can limit tree growth by restricting oxygen availability or causing water stress.

2.1.3 pH

Soil pH is another fundamental parameter, as it governs the chemical environment of the soil. It directly affects the availability of nutrients to plants and regulates microbial activity. Most nutrients are optimally available within a moderate pH range (between 6 and 7 [17]), and extreme acidity or alkalinity can limit plant uptake and growth [18].

2.1.4 Soil organic carbon

Soil organic carbon improves the physical properties of the soil. It increases the cation exchange capacity (CEC) and the water-holding capacity and it contributes to the structural stability of clay soils by helping to bind particles into aggregates. Soil organic matter, of which carbon is a major part, holds a great proportion of nutrients, cations and trace elements that are of

importance to plant growth. It prevents nutrient leaching and is integral to the organic acids that make minerals available to plants. It also buffers soil from strong changes in pH. It is widely accepted that the organic carbon content of the soil is a major factor in its overall health, is a major part of the Carbon Cycle and an important factor in the mitigation of climate change effects [19].

2.1.5 Phosphorus

Available phosphorus is a critical parameter, as it is often a limiting nutrient. It plays a key role in root development, energy transfer, and overall plant growth, and low availability can restrict tree establishment [20].

2.1.6 Macronutrients

Macronutrients such as potassium (K), which is required in large amounts for plant development [21], was expected to be more abundant in productive soils. Similarly, secondary nutrients such as calcium (Ca), magnesium (Mg), and sulphur (S) play essential roles in plant structure and metabolic processes, and should therefore also be present in sufficient quantities in fertile soils.

2.1.7 Trace metals

Trace metals like iron (Fe), manganese (Mn), zinc (Zn), copper (Cu), although required in smaller amounts, are crucial for various physiological functions, and were likewise expected to be found in adequate concentrations in high-quality soils.

3 Methods

The work began with an in-depth literature review 1.2 focusing on tropical soil dynamics, the determinants of natural regeneration and the impact of slash-and-burn agriculture on soil fertility. This stage allowed for the precise definition of research hypotheses and guide the experimental protocol in the context of Guinea.

3.1 Presenting the samples

The high-performing and low-performing parcels for tree regeneration have been determined from the data provided by arboRise Foundation. The dataset comprises various information about the plots, such as the details of the trees present in each plot, including their number, species, diameter, height, carbon content, and wood density and biomass. The data on tree biomass in the parcels is based on the forest inventory realized between October and December 2025 on the 116 monitoring plots spread among the 840 reforested plots, following the methodology of The Gold Standard, one of the most demanding carbon certification standard. The methodology requires the measurement of the diameter at breast height (DBH) and identification of the species of all trees above 2 meters within the 625 sqm of each monitoring plot. The trees that were already present on the parcels, before the arboRise plantation took place are called the baseline trees. They were excluded from the calculation of produced biomass. The parcels have been planted with trees in different years and are currently in different stages of regeneration, which was taken into account implicitly in the calculation of produced biomass. The equation for the calculation of the biomass for a single tree is the following :

$$\text{Biomass} = \exp(-1.8623 + 2.4023 \cdot \ln(\text{DBH}) - 0.3414 \cdot \ln(\rho)) [22],$$

where DBH is the diameter at breast height of the tree and ρ is the density of the tree. The biomass values were then computed for all of the parcels, considering the proportion of all the different species present there.

In total, soil samples from 19 plots were collected, 9 of them were collected from identified low-productivity plots and 10 from high-productivity plots. The protocol is described in the paragraph 3.2. The parcels with the lowest biomass values from all parcels represent the low-productivity parcels and the ones with the highest biomass values correspond to the high-productivity parcels.

The coordinates of the parcel centers, along with the plot IDs, the biomass content in trees expressed in kgCO₂ and the name of the nearby villages can be visualised below in Table 1. As it can be seen, the range of the biomass content varies greatly, from 11 kgCO₂ to 205 kgCO₂, indicating strong variability across the studied parcels. The locations of the plots can be visualised in the context of Guinea on Figure 1 and the region on interest in the East of Guinea on Figure 2.

Table 1: Soil sampling locations and biomass

Village	Plot ID	Biomass	Latitude	Longitude
FORONO	2023-076	11	9,4305	-8,6781
MAMOUROU.	2024-163	12	9,2419	-8,7103
KOFILAKORO	2023-085	13	9,4003	-8,6849
KOFILAKORO	2022-013	26	9,4156	-8,6950
FANSAN	2024-194	29	9,3302	-8,7744
FANSAN	2024-097	57	9,3217	-8,7835
FANSAN	2021-047	59	9,3306	-8,7972
DIARAGBER.	2023-257	63	9,3356	-8,6790
LINKO	2022-138	83	9,3855	-8,8240
FANSAN	2022-173	102	9,3228	-8,7833
FANSAN	2023-253	123	9,3268	-8,7741
SEMANDOU	2021-064	128	9,2609	-8,7472
FORONO	2022-020	135	9,4389	-8,6694
DEYLA	2024-119	138	9,3456	-8,7303
LINKO	2024-206	151	9,3831	-8,8233
LINKO	2021-002	177	9,3924	-8,8034
LINKO	2022-149	189	9,3857	-8,8054
FORONO	2022-018	195	9,4259	-8,6638
LINKO	2021-005	205	9,3753	-8,7993

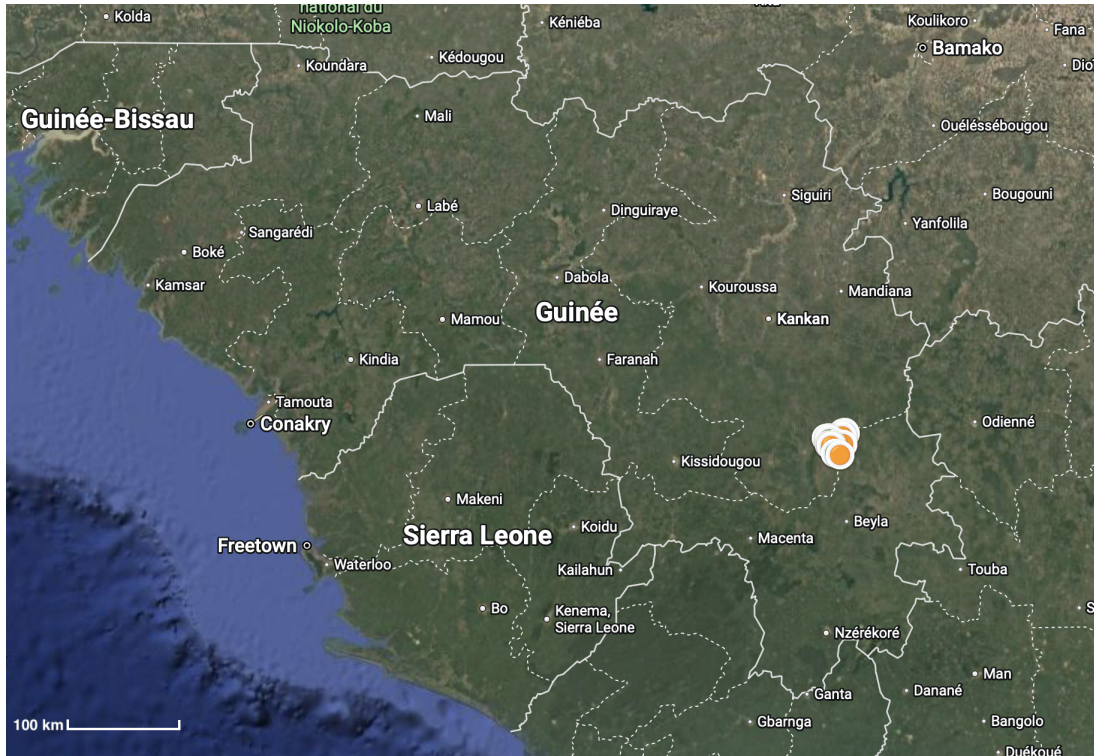


Figure 1: Locations of parcels in the context of Guinea

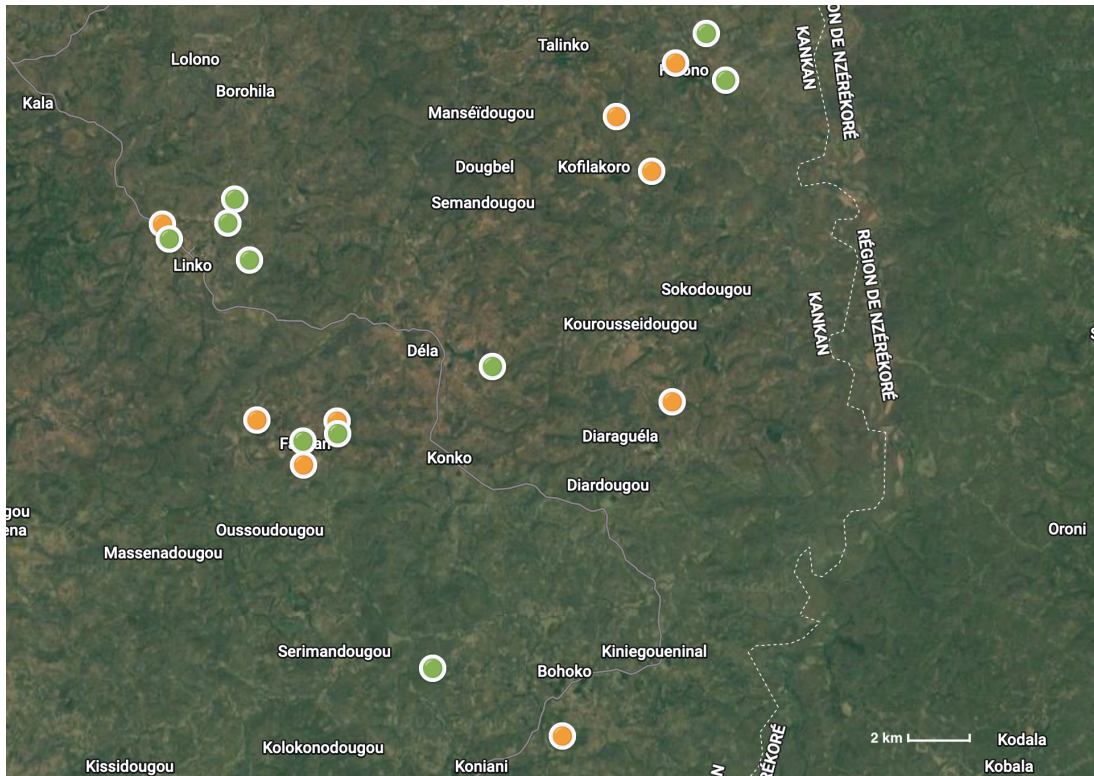


Figure 2: Locations of assumed high-productivity/good parcels (in green) and low-productivity/bad parcels (in orange)

3.2 Sample collection

In order to collect soil samples in a rigorous and standardized manner, a dedicated field sampling protocol was developed. The protocol targets plots that have exhibited significantly high and

low biomass production since the ArboRise plantations, excluding pre-existing trees. For each selected plot, approximately 100 g of soil is collected at three distinct locations using a hoe, at a depth ranging from 10 to 40 cm. Three sampling points are carefully selected to obtain a sample as representative as possible of the overall soil conditions of the parcel. The three subsamples are then combined to form a composite sample of approximately 300 g, which is sealed in double airtight plastic bags, labeled with the plot code using a permanent marker, and placed in rigid containers for transport. This procedure is repeated systematically for each plot, with predefined replacement plots available should a given parcel prove inaccessible or unsuitable for sampling. This protocol ensured that soil samples were collected in a consistent manner, providing a basis for subsequent laboratory analyses.

3.3 Sample laboratory analysis

3.3.1 Stone content and soil color

First, the parcels were visually evaluated to assess differences in soil color and apparent stone content. The weight or proportion of stones present in the soil samples was not quantitatively measured during this study. Instead, soils were classified according to their visible stone content, distinguishing between parcels with relatively high, moderate, or low amounts of stones. As these observations were based solely on visual inspection and not on empirical measurements, they should be considered qualitative assessments intended only to provide a comparative indication of the relative stoniness of the different soil samples.

3.3.2 Particle size distribution

In order to determine soil texture, the prepared soil of < 2 mm of diameter, is sieved through 2 sieves, the first one with a mesh size of 0.2 mm (or $200\mu m$) and the second one with a mesh size of 0.05 mm (or $50\mu m$). The first sieve only lets pass fine sand and smaller particles and the second one lets pass silt and clay particles, thus separating the soil into three fractions : silt and clay, fine sand and coarse sand.

3.3.3 Moisture Content

All the glass jars were first weighed without their lids to determine their initial mass. The jars were then filled with soil and weighed again without the lids. Afterwards, the jars were dried in an oven at $105\text{ }^{\circ}\text{C}$ for 24 hours and weighed once more after drying. The moisture content was calculated using the following equation :

$$\text{Moisture Content (\%)} = 100 - \frac{m_{\text{jar with dried soil}} - m_{\text{empty jar}}}{m_{\text{jar with moist soil}} - m_{\text{empty jar}}} \cdot 100$$

As the soil samples were transported in plastic bags rather than sealed containers, moisture loss through evaporation cannot be ruled out. Furthermore, their water content may vary depending on the meteorological conditions preceding sampling. These two factors introduce potential inaccuracies that may compromise the reliability of the results.

3.3.4 pH

Using a spatula, 6 ± 0.1 g of soil sample was weighed and put into centrifuge tubes. 15 mL of deionized water was added to each tube using a graduated cylinder. The tubes were sealed and placed on an agitation table at low speed for 30 minutes, after which the suspension was allowed to decant for a further 30 minutes.

To measure pH, the electrode tip was inserted into the supernatant, ensuring it was fully submerged without touching the slurry at the bottom of the tube. Once a stable reading was obtained, the electrode was rinsed with deionized water and gently blotted dry. This procedure was repeated for each sample. At the end of each batch, the pH of the first sample was re-measured to verify the absence of drift.

3.3.5 Soil Organic Carbon

Prior to analysis, soil samples were dried and sieved before being transferred grinding jars filled with beads. Samples were ground using a ball mill at 600 rpm for 3 minutes, producing a fine homogeneous powder. After grinding, the powder was recovered by sieving the jar contents into a plastic boat and scraping the jar walls with a plastic spatula to ensure complete sample recovery. Total carbon concentrations were subsequently measured on the resulting powder using a TOC analyser.

3.3.6 Macronutrients and trace metals

X-ray fluorescence (XRF) analysis is used to determine the elemental composition of the soil, including macronutrients and micronutrients as well as potential contaminants. This technique provides insight into the mineralogical composition and helps identify nutrient deficiencies or toxic elements that may affect tree growth [23]. More specifically, the Geochemistry Traces Powders method is employed, measuring elemental concentrations in powdered soil samples (already made for soil organic carbon analysis :subsubsection 3.3.5), with results expressed in $\mu\text{g/g}$ (ppm).

3.4 Multivariate analysis

Unsupervised clustering methods are in general applied to identify natural groupings or gradients within the dataset without prior assumptions or predefined labels. These methods rely on the internal structure of the data and depend on the choice of distance metric and clustering algorithm. Prior to clustering, all variables must be standardized to ensure comparability between different units and scales.

The method that is used for this project is the Principal Component Analysis (PCA) is used to reduce the dimensionality of the dataset by transforming correlated variables into a smaller number of uncorrelated components. This will help identify the main gradients in soil composition and facilitate the interpretation of relationships between soil properties and tree biomass.

4 Results

4.1 Stone content and soil color

Table 2 highlights visible differences in soil color and apparent stoniness among the studied parcels. As stone content was not quantitatively measured, these observations are presented solely as qualitative descriptions to compare the parcels between them.

Table 2: Field Observations

Parcel ID	Field observation	Color
2023-076	Few stones	Brown
2024-163	Medium stones	Dark brown
2023-085	Many stones and roots	Brown
2022-013	Medium stones	Red
2024-194	Medium stones	Brown
2024-097	Medium stones	Red brown
2021-047	Many small stones	Brown
2023-257	Few stones	Red brown
2022-138	Medium stones	Grey brown
2022-173	Few to medium stones	Brown
2023-253	Medium small stones	Brown
2021-064	Few stones	Dark brown
2022-020	Medium stones	Brown
2024-119	Almost no stones, granular	Light brown
2024-206	Many small stones	Grey brown
2021-002	Few stones	Red brown
2022-149	Few to medium stones	Dark brown
2022-018	Medium stones	Brown
2021-005	Medium stones	Brown

The soils with lower productivity tended to display a more pronounced red coloration and a lower stone quantity.

4.2 Particle size distribution

The fraction of the types of particles in each parcel can be found in Table 3.

Table 3: Grain Size Distribution – Fraction of Total Mass (%)

Parcel ID	Coarse sand > 200 μm	Fine sand 50–200 μm	Silt and clay < 50 μm
2023-076	79,19	20,35	0,46
2024-163	80,85	18,09	1,06
2023-085	96,05	3,24	0,71
2022-013	81,92	17,85	0,23
2024-194	80,24	18,72	1,04
2024-097	82,08	16,74	1,18
2021-047	78,24	20,65	1,11
2023-257	81,18	17,93	0,89
2022-138	77,06	22,60	0,34
2022-173	83,50	15,76	0,74
2023-253	75,81	22,00	2,18
2021-064	95,74	3,66	0,60
2022-020	83,76	13,89	2,35
2024-119	78,75	20,83	0,42
2024-206	78,52	18,69	2,79
2021-002	80,62	16,41	2,97
2022-149	66,64	31,27	2,10
2022-018	87,74	10,91	1,35
2021-005	87,22	12,15	0,63

Less productive soils show a mean silt and clay fraction of 0.78% of total mass, compared to 1.62% for the most productive ones, meaning productive soils contain more than twice the proportion of finest particles. This difference is clearly visible in Figure 4.

Figure 3 shows the mass fraction of particles in a more visual way. Coarse sands take up most of the mass fraction, followed by fine sands and silt and clay.

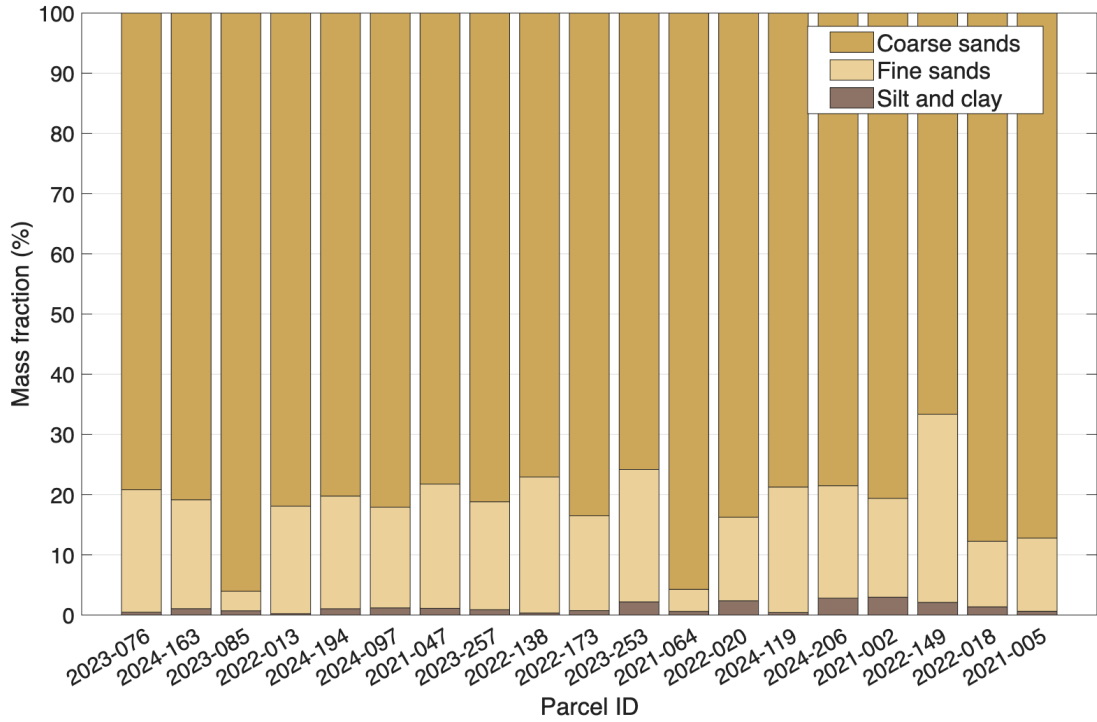


Figure 3: Particle size distribution in parcels

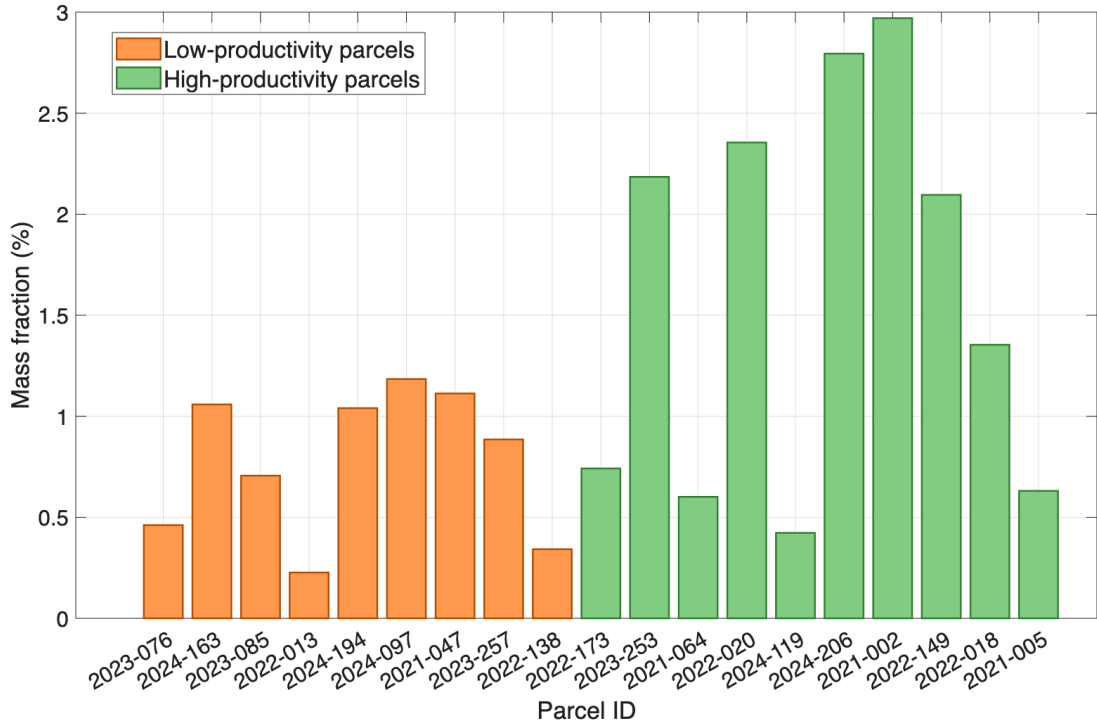


Figure 4: Silt and clay mass fractions in parcels

4.3 Moisture content

The moisture content of each parcel can be visualized in the Table 4. The results don't show a clear difference between high-performing and low-performing parcels indicating no relation between the type of parcel and the moisture content.

Table 4: Moisture Content

Parcel ID	Moisture Content (%)	Parcel ID	Moisture Content (%)
2023-076	3,45	2022-173	5,77
2024-163	2,84	2023-253	7,48
2023-085	13,40	2021-064	4,15
2022-013	15,21	2022-020	5,12
2024-194	11,46	2024-119	9,10
2024-097	9,56	2024-206	0,96
2021-047	6,13	2021-002	9,41
2023-257	10,68	2022-149	4,81
2022-138	8,24	2022-018	6,07
		2021-005	5,45

4.4 pH

Table 5: Soil pH

Parcel ID	pH	Parcel ID	pH
2023-076	5,48	2022-173	5,45
2024-163	5,78	2023-253	5,62
2023-085	5,49	2021-064	6,20
2022-013	5,43	2022-020	6,17
2024-194	5,44	2024-119	5,48
2024-097	5,43	2024-206	5,87
2021-047	5,90	2021-002	6,01
2023-257	5,36	2022-149	6,15
2022-138	5,57	2022-018	5,87
		2021-005	6,12

The results of pH measurements in Table 5 suggest a moderate but consistent difference in soil pH between productivity classes. Less productive soils display a mean pH of 5.54, while more productive soils show a higher mean of 5.89.

4.5 Soil organic carbon

The total carbon content of each parcel can be visualised in the Table 6.

Table 6: Soil total carbon

Parcel ID	Total Carbon (%)	Parcel ID	Total Carbon (%)
2023-076	1,13	2022-173	1,07
2024-163	1,69	2023-253	1,43
2023-085	1,70	2021-064	1,28
2022-013	1,45	2022-020	1,23
2024-194	1,91	2024-119	0,89
2024-097	2,27	2024-206	0,92
2021-047	0,88	2021-002	1,72
2023-257	1,64	2022-149	1,10
2022-138	0,68	2022-018	0,83
		2021-005	0,99

The results show a counterintuitive trend: less productive soils exhibit a higher mean total carbon content (mean of 1.48%) compared to more productive soils (mean of 1.15%).

The Figure 5 demonstrates the plot of Total Carbon against the year of the parcel plantation, in order to see if the age of the parcel has to do with the amount of carbon in it. Even though the regression line of the TC follows an increasing trend, it appears that the TC and years of the parcel have no correlation, with a p-value > 0.05 and a Pearson correlation coefficient of 0.39. This means that the parcels are comparable, independently of their year of planting, in terms of carbon content.

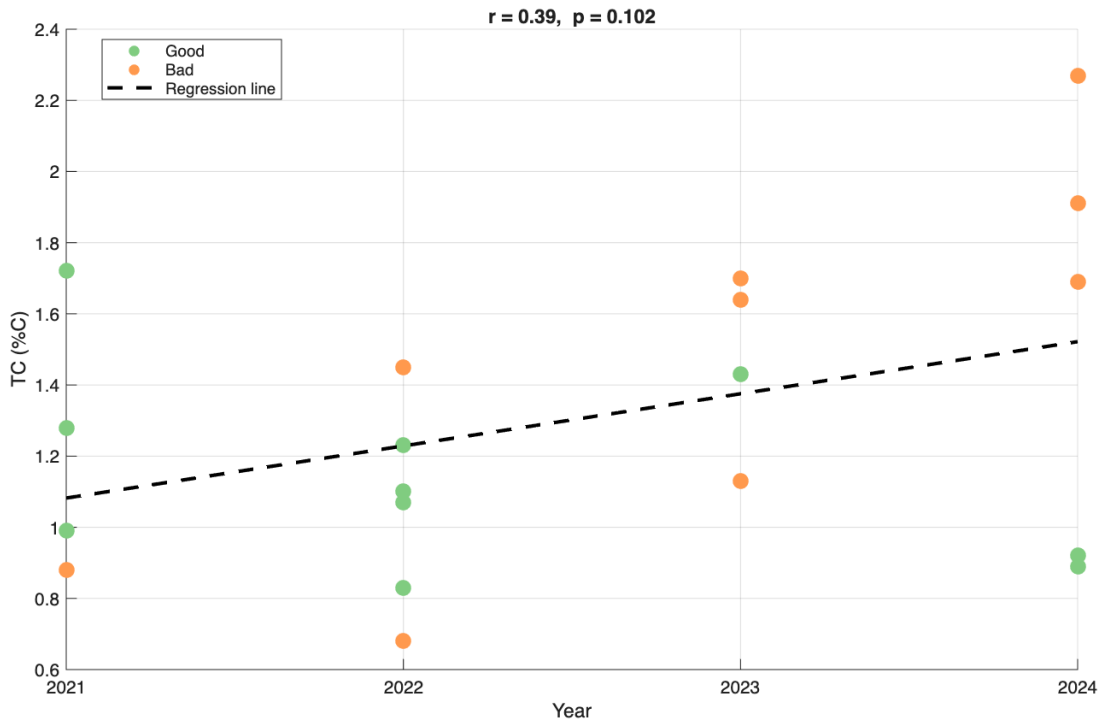


Figure 5: Year of planting vs Total Carbon (TC)

4.6 Macronutrients and Trace metals

Phosphorus The phosphorus concentration of each parcel can be visualised in the Table 7.

Table 7: Soil phosphorus

Parcel ID	Phosphorus ($\mu\text{g/g}$)	Parcel ID	Phosphorus ($\mu\text{g/g}$)
2023-076	518	2022-173	453
2024-163	566	2023-253	458
2023-085	480	2021-064	386
2022-013	551	2022-020	570
2024-194	678	2024-119	257
2024-097	714	2024-206	369
2021-047	445	2021-002	631
2023-257	480	2022-149	504
2022-138	372	2022-018	182
		2021-005	432

Interestingly, the results show a counterintuitive trend regarding phosphorus content: less productive soils exhibit a higher mean phosphorus concentration ($533.7 \mu\text{g/g}$) compared to more productive soils ($424.0 \mu\text{g/g}$).

Other macronutrients The element concentrations of each parcel can be visualised in the Table 8.

Table 8: Element concentrations ($\mu\text{g/g}$) in soil samples

Parcel ID	K	Ca	Mg	S	Fe	Mn	Zn	Cu
2023-076	1333	594,9	1295	179,4	61790	305	22,9	25,9
2024-163	3139	917,4	861	233,7	60900	502	26,1	20
2023-085	1617	610,4	647	209,1	96070	579	33,6	66
2022-013	2035	346,4	852	172,5	74880	432	27,1	46,3
2024-194	1626	415,1	1368	217,2	146600	960	31,3	103,2
2024-097	1508	522,7	1352	231,9	151200	1218	36	109,5
2021-047	4360	420,8	644	167	54870	504	29,9	24,5
2023-257	1616	411,3	614	210,5	84980	306	30,8	159,4
2022-138	5468	374	740	151,9	32770	283	18,7	15,7
2022-173	1692	451,2	1368	182	53740	352	22,7	35,5
2023-253	1567	460,3	956	235,8	92050	375	22,9	52,2
2021-064	2261	1653	1093	219,6	35980	680	23,6	28,9
2022-020	3886	905,7	1339	198,7	91650	781	26,5	41,2
2024-119	2446	520,2	634	147,1	37290	124	24,9	31,2
2024-206	18260	553,7	790	177,9	20750	257	13,6	7,3
2021-002	1966	837,2	1043	218,7	92540	1098	33,2	114,8
2022-149	20110	2620	2566	214,8	33980	664	26,7	23,6
2022-018	3418	348,3	627	273,9	42980	396	17,3	25,2
2021-005	13780	2019	1720	182,6	48890	864	27,7	27,4

Among these elements, potassium shows the most striking contrast between groups. Mean K concentration in high-productivity parcels reaches $6938 \mu\text{g/g}$, nearly three times the value recorded in low-productivity parcels ($2522 \mu\text{g/g}$). This difference is largely driven by three high-productivity parcels (2024-206, 2022-149 and 2021-005) displaying exceptionally elevated K values of 18260, 20110 and $13780 \mu\text{g/g}$ respectively (Table 8). Outside of these outliers, K levels are broadly comparable between groups, suggesting that potassium distribution across the study area is heterogeneous.

Calcium shows a more consistent pattern, with high-productivity parcels averaging $1037 \mu\text{g/g}$, which is more than twice as high as $513 \mu\text{g/g}$ in low-productivity parcels. Magnesium follows a similar but more moderate trend, with mean values of $1214 \mu\text{g/g}$ in high-productivity parcels versus $930 \mu\text{g/g}$ in low-productivity parcels. The high-productivity parcel 2022-149 stands out, with an exceptionally high Mg value of $2566 \mu\text{g/g}$.

Sulfur, by contrast, shows virtually no difference between groups, with mean concentrations of $197 \mu\text{g/g}$ in low-productivity parcels and $205 \mu\text{g/g}$ in high-productivity parcels.

Figure 6 shows the concentrations normalized by means of the four different macronutrients. The parcels that stand out once again are the good parcels 2022-149 and 2021-005, which both have high concentrations of calcium, magnesium and sulfur.

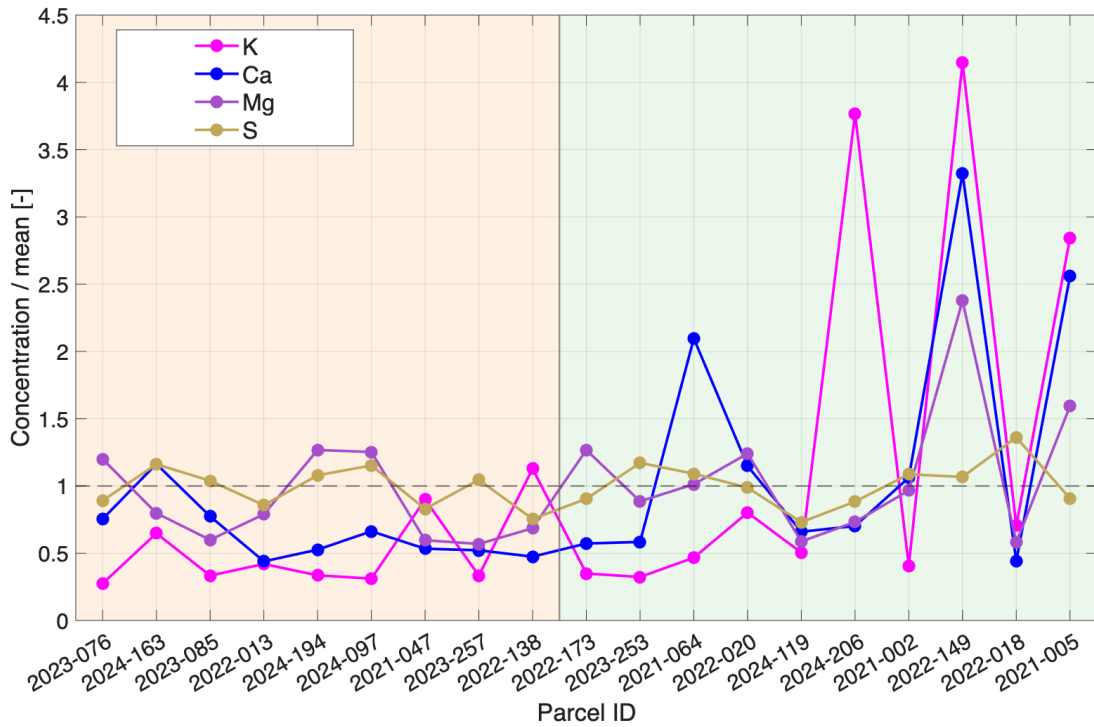


Figure 6: Macronutrients (concentrations normalized by mean) in each parcel

The values of pH are plotted against the calcium concentrations, in order to examine their relationship. Figure 7 shows a **clear correlation between pH and Ca**, with $p < 0.05$ and a Pearson correlation coefficient of 0.71. Bad parcels have rather low values of Ca and pH and good parcels generally show higher values for both.

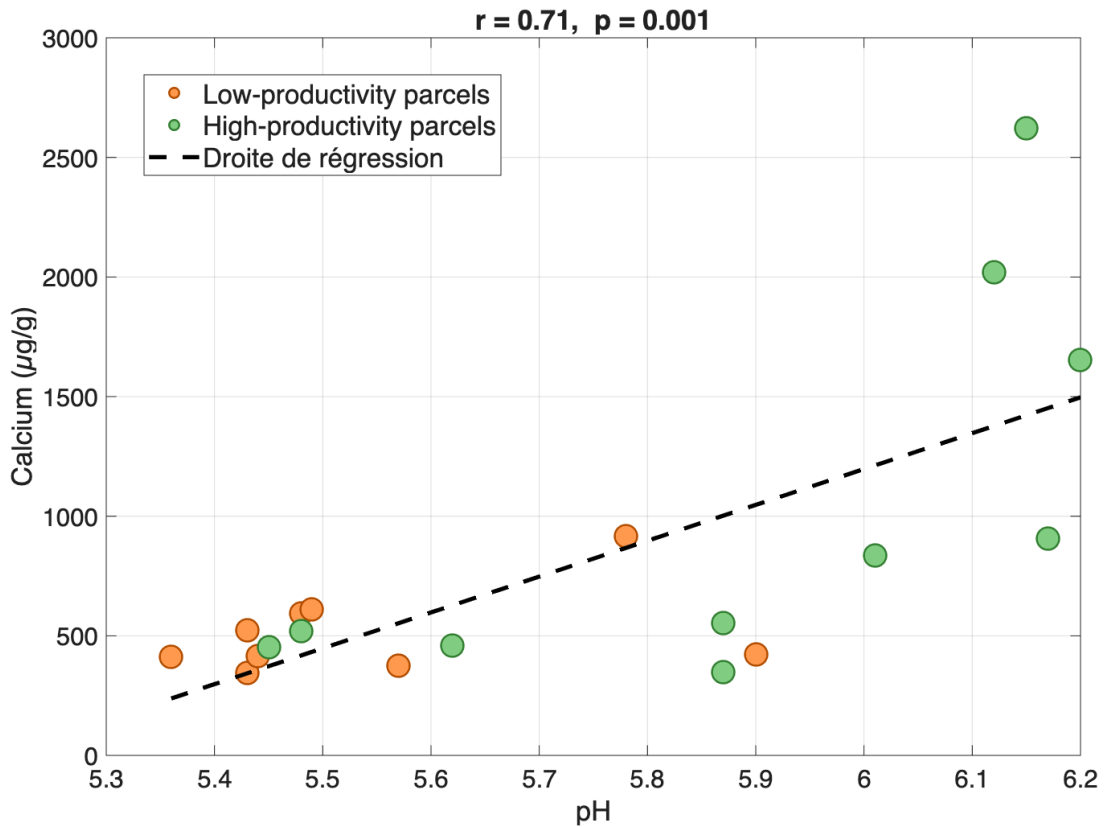


Figure 7: pH vs Calcium concentration ($\mu\text{g/g}$)

Trace Metals The analysis of transition metals across the sampled parcels reveals contrasting patterns depending on the element considered (Table 8). Iron (Fe) shows the most striking difference between groups, with a mean concentration of $84896 \mu\text{g/g}$ in the low-productivity parcels compared to $54985 \mu\text{g/g}$ in the high-productivity parcels, a difference of approximately 54%. Copper (Cu) similarly shows higher mean values in low-productivity parcels ($63.4 \mu\text{g/g}$) than in high-productivity parcels ($38.7 \mu\text{g/g}$).

In contrast, manganese (Mn) and zinc (Zn) show no meaningful difference between the two groups. Mean Mn concentrations are nearly identical ($566 \mu\text{g/g}$ in low-productivity parcels versus $559 \mu\text{g/g}$ in high-productivity parcels), and Zn values are uniformly low across all sites (28.5 versus $23.9 \mu\text{g/g}$). While Mn levels are elevated in absolute terms, with several parcels exceeding $900 \mu\text{g/g}$, they do not appear to discriminate between soil quality classes in this dataset.

Figure 8 demonstrates the concentrations of the trace metals normalized by their respective mean concentrations, in order to see whether they have similar trends. In general, all four metals are higher or lower than the unit measure for the same parcels. It is especially visible for low-productive parcels 2024-194, 2024-097 and good parcels 2024-206 and 2021-002.

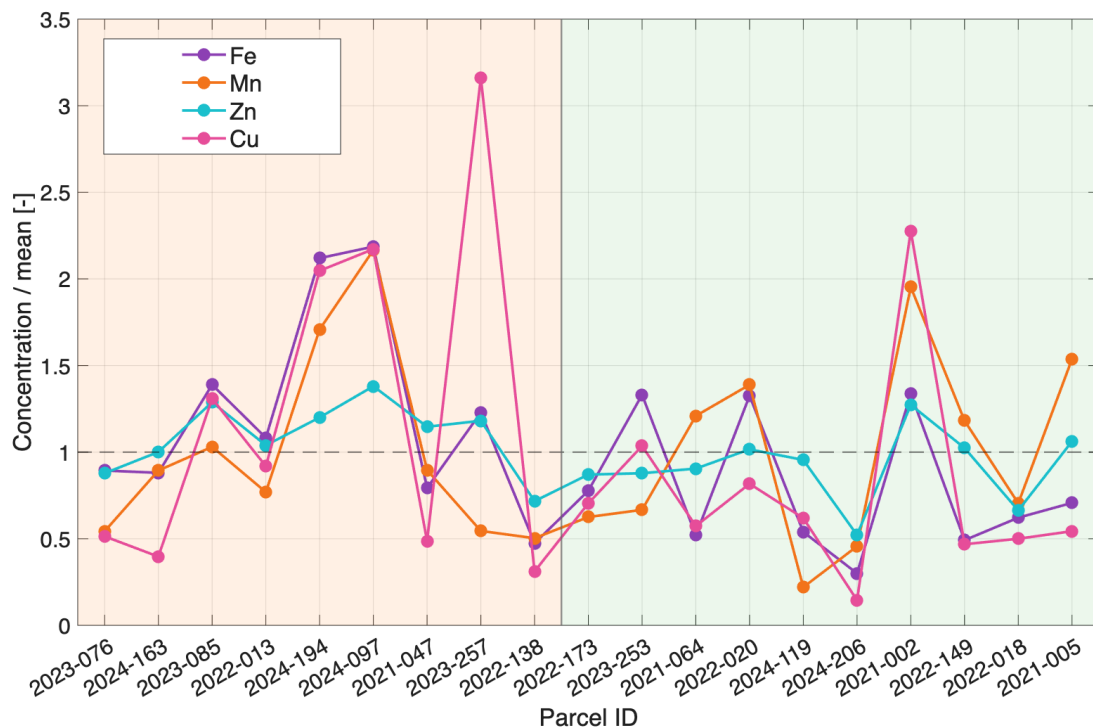


Figure 8: Trace metals (concentrations normalized by mean) in each parcel

4.7 Multivariate Analysis

Biplot on Figure 9 overlays the parcels (little dots) and the parameters (lines). It takes into account the following parameters : biomass, pH, moisture content, granulometrics (fine sand, silt and clay), TC (total carbon) and XRF results (P, K, Ca, Mg, S, Fe, Mn, Zn, Cu). The ratio of coarse sands isn't taken into account, because PCA works with independent variables and coarse sands ratio depends directly on the ratio of fine sands and silt and clay. The direction in which the arrows point tells us about their correlation. The two axes correspond to PC1 and PC2. PC1 and PC2 are artificial axes that were created from the original variables. PC1 explains the largest amount of variation in the data and PC2 explains the second largest amount of variation and is independent from PC1.

The parameters on the right of the plot point in the same direction, which means that they

are correlated. A parcel with a high PC1 score, on the right of the plot, has a higher content in trace metals (Fe, Mn, Zn, Cu), organic matter (total carbon), moisture content and some macronutrients (P, S) and a lower pH and content in some macronutrients (Mg, Ca, K), in silt and clay and fine sands (so a higher content in coarse sands) and finally, a lower biomass. A parcel with a high PC2 score has a higher amount of all parameters, except for the moisture content. Essentially, this means that in terms of PC1 the parameters on the right of the plot are all correlated with each other and the ones on the left are all correlated between them. In terms of PC2, all parameters are correlated between them, except for moisture content.

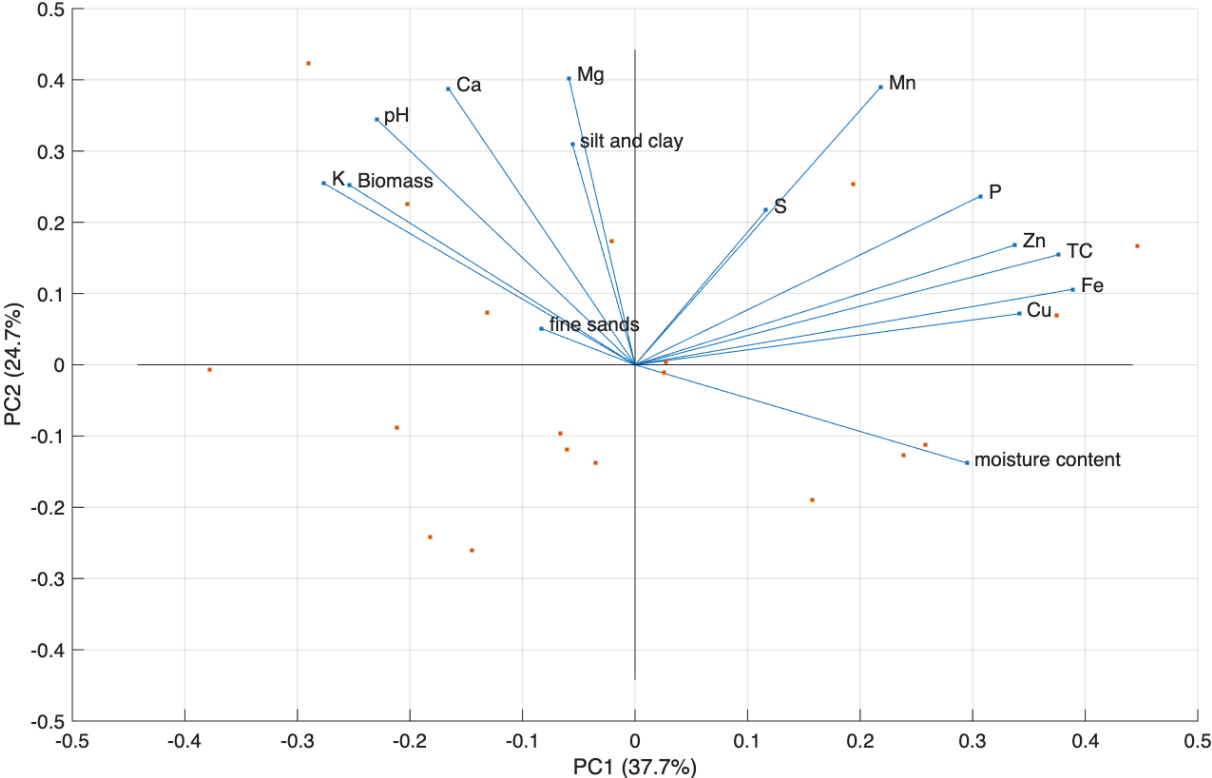


Figure 9: PCA Biplot

The PCA Score Plot on Figure 10 is used to see whether there is a natural clustering of good and bad parcels between them. It takes into account all of the parameters, as in the plot in Figure 9, except for the biomass. We want to see if high-performing and, similarly, low-performing parcels are drawn towards each other in terms of the measured parameters only.

PC1 separates good from bad parcels quite well, bad parcels (in orange) cluster on the right, indicating a high PC1. The bad parcels 2024-097, 2024-194, 2023-085, 2023-257, 2022-013 have high metal, TC, and moisture content. When referring to Table 5, they in fact all have a pH < 5.5. Good parcels (in green) cluster on the left-center. The parcels 2021-005, 2022-020, 2021-002 and 2021-064 all have a pH > 6 (Table 5). There are still some exceptions, the parcels 2022-149 (good, top-left) and 2024-206 (good, far left) are outliers worth investigating.

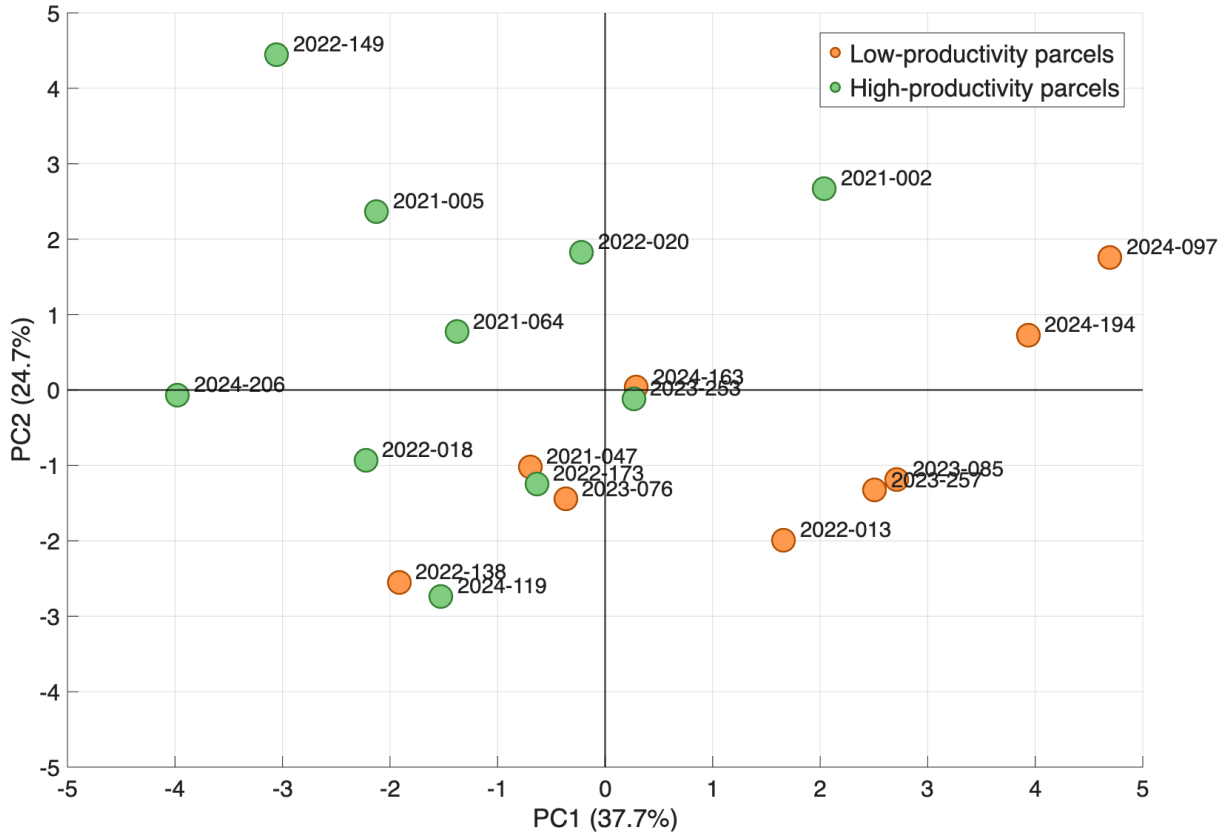


Figure 10: PCA Score Plot

5 Discussion

The results of this study reveal a consistent pattern in which soil pH emerges as a central driver of tree growth performance across the studied parcels. Good parcels display a mean pH of 5.89 compared to 5.54 for bad parcels (subsection 4.4). Both groups fall within the acidic range, which is typical of highly weathered tropical soils. However, the more productive soils tend toward a less acidic pH, which favors greater nutrient availability, particularly phosphorus, whose solubility and plant uptake are strongly reduced below pH 5.5 [24]. This threshold is notably approached or exceeded by several samples in the less productive group, which could contribute to nutrient limitations and partly explain the observed differences in biomass growth. Below pH 5.5, phosphorus becomes strongly bound to iron and aluminium oxides [24], making it largely unavailable for plant uptake despite its relatively high total concentration in the soil. This mechanism likely explains the counterintuitive finding that less productive soils actually contain higher total phosphorus concentrations (533.7 $\mu\text{g/g}$ versus 424.0 $\mu\text{g/g}$, subsection 4.6). The phosphorus is present but inaccessible, fixed by the acidic soil chemistry rather than available for biological uptake. This highlights the importance of interpreting phosphorus data in conjunction with pH measurements, and suggests that phosphorus fixation could be a significant limiting factor in the less productive soils.

This interpretation is further supported by the observed relationship between pH and calcium. The significant positive correlation between pH and Ca ($p < 0.05$, Figure 7) suggests that soils with higher calcium content tend to be less acidic. Given that Ca^{2+} is one of the base cations most readily lost through leaching in tropical soils, its depletion in low-productivity parcels is consistent with a more advanced stage of soil acidification and weathering. Calcium and magnesium, which are among the base cations responsible for maintaining soil pH, are progressively lost through leaching in highly weathered tropical environments. Their depletion leads to increased soil acidity, which in turn further reduces the availability of other nutrients including phosphorus

and potassium. This means that pH is not just one parameter among many, but an important indicator of the overall chemical fertility of these soils.

The homogeneity of sulfur between different parcels (subsection 4.6) suggests that S cycling is not a differentiating factor between soil quality classes in this dataset, and that sulfur presence is unlikely to be a limiting factor for reforestation in either group. Taken together, the macronutrient data point to a consistent pattern of base cation depletion, particularly Ca and to a lesser extent Mg, in low-productivity parcels, which aligns with the hypothesis of greater weathering intensity and acidification in these soils. The marked K enrichment in a subset of high-productivity parcels further suggests that geological heterogeneity plays a role in shaping fertility differences across the study area.

In terms of trace metals, such elevated Fe levels in low-productivity soils are consistent with the geochemical characteristics of highly weathered tropical soils, where iron oxides and hydroxides accumulate as a result of intense leaching of other elements, a process known as ferralitisation. High Fe concentrations are also known to induce phosphorus fixation, whereby Fe oxides adsorb phosphate ions and render them unavailable to plants, a mechanism that could partly explain reduced fertility in the low-productivity parcels. Low-productivity parcels have rather high levels of copper, with some the Swiss OSITES indicative threshold of 40 mg/kg, and one parcel reaching 159 $\mu\text{g/g}$, approaching the remediation threshold of 150 mg/kg [25]. **This elevated Cu in low-productivity soils may reflect anthropogenic inputs.** Mn concentrations are relatively low in all analyzed samples and show no particular pattern or systematic variation among the studied sites. This results suggest that Mn distribution could be primarily driven by the shared geological parent material rather than by degradation processes. Zinc levels present no contamination concern in either group. Taken together, these results suggest that Fe and Cu are the most informative metals in differentiating low-productivity from high-productivity soils in this study, while Mn and Zn appear largely homogeneous across sites. The strong Fe enrichment in low-productivity parcels, combined with elevated Cu in the same group, points toward a combination of pedogenic processes and potential anthropogenic pressures that may contribute to reduced soil quality and tree growth potential.

The PCA confirms and further supports these findings (subsection 4.7). PC1, which explains 38.3% of total variance, clearly separates good from bad parcels along a gradient opposing trace metals and organic carbon on one side against base cations (Ca, Mg, K) and pH on the other. Bad parcels cluster on the positive side of PC1, characterised by elevated Fe, Cu, Mn, TC and moisture content. Good parcels cluster on the negative side of PC1, with relatively higher pH, Ca, Mg, and K, pointing toward a more favourable chemical environment for nutrient uptake and root development.

The particle size results add a complementary physical dimension to this picture. Good parcels contain on average more than twice the proportion of silt and clay (1.62% versus 0.78%) subsection 4.2, which enhances cation exchange capacity, water retention, and nutrient holding. This is consistent with the observed higher calcium and magnesium concentrations in productive soils: fine particles provide a larger specific surface area and contribute to a higher cation exchange capacity (CEC), a property that enables soil particles to retain and exchange essential plant nutrients such as potassium (K^+), calcium (Ca^{2+}), and magnesium (Mg^{2+}) [26] rather than allowing them to be leached from the root zone. Furthermore, the smaller pore spaces associated with silt and clay enhance the soil's capacity to store water [27], providing a more stable supply of moisture during periods of limited rainfall. Together, these characteristics create more favorable growing conditions that can support greater plant growth and ultimately higher biomass productivity. The two gradients, chemical fertility driven by pH and base cations, and physical texture driven by fine particle content, therefore appear to be mutually reinforcing factors explaining tree growth performance across the studied parcels.

Total carbon content does not follow the expected pattern, with less productive soils showing a higher mean carbon content (subsection 4.5). This finding may seem paradoxical, as higher organic carbon is generally associated higher biomass production. However, several explanations may account for this pattern in the context of tropical reforestation plots. First, the less productive parcels may correspond to plots that have been under fallow for longer or more recently abandoned, allowing organic matter to accumulate without being actively cycled through vegetation. In contrast, more productive parcels with greater tree establishment may be in an active phase of organic matter decomposition and nutrient uptake, where carbon is being rapidly mineralised and incorporated into biomass rather than stored in the soil. Second, total carbon content does not distinguish between stable, recalcitrant carbon fractions and labile, biologically active organic matter. Soils with similar or higher total carbon values can therefore differ substantially in the fraction that is actually available to support microbial activity and plant growth, which means that total carbon alone is not necessarily a reliable indicator of soil biological quality. Finally, it should be noted that the differences between the two groups remain modest and overlap considerably, suggesting that total carbon alone may not be a decisive driver of productivity in these soils. Other parameters are likely to play a more determining role in explaining the observed variability in tree growth across parcels.

Overall, the convergence of evidence from particle size analysis, pH measurements, elemental concentrations, and multivariate analysis suggests that the primary limiting factor for tree growth in these parcels is not nutrient quantity, but nutrient availability, which is governed above all by soil pH. Soils that are too acidic lock up phosphorus, lose base cations through leaching, and may accumulate toxic levels of soluble iron and manganese. Addressing soil acidity therefore appears to be the most critical intervention for improving reforestation outcomes in this region.

5.1 Recommendations

Soil pH should be measured in all sites candidate for arboRise’s reforestation programs as strongly acidic soils ($\text{pH} < 5.5$) could severely compromise tree establishment and growth. It is therefore recommended to either exclude the most acidic sites from reforestation programs, or to treat them prior to planting. Treatment could be made through liming through the application of agricultural limestone (CaCO_3) or dolomitic lime ($\text{CaMg}(\text{CO}_3)_2$) [28].

The incorporation of organic matter through composting, green manures, agroforestry leaf litter, or biochar application can significantly improve soil quality and complement liming strategies. Organic amendments increase soil organic carbon content, enhance soil structure, improve water retention, and increase the soil’s buffering capacity, thereby reducing aluminum toxicity and making pH correction more durable over time [9]. Among these amendments, biochar has attracted considerable attention due to its unique physicochemical properties. It is a carbon-rich material characterized by a high specific surface area, elevated cation exchange capacity, and remarkable stability in soil [29]. These properties allow biochar not only to contribute to long-term carbon sequestration and nutrient retention but also to increase soil organic matter stocks and improve the effectiveness of other organic amendments such as compost. Furthermore, biochar can help neutralize soil acidity and increase soil pH, particularly in acidic soils [30]. As a result, biochar application has been associated with improvements in nutrient availability, water-holding capacity, microbial activity, and overall soil fertility [29]. Given its ability to simultaneously influence multiple key soil properties biochar may represent a particularly promising strategy for improving soil productivity in a holistic and sustainable manner.

Places where access to industrial lime is limited by cost or supply constraints, locally available amendments offer viable alternatives. Wood ash [12] could represent a low-cost and practical option in the Guinean context. It can raise soil pH effectively while simultaneously supplying potassium, calcium, and magnesium at very low cost. It is recommended to apply the liming material at least three to six months before the growing season allowing sufficient time for pH

stabilization [31].

5.2 Limitations

The primary limitation of this study is the relatively small sample size. Although each sample consists of soil collected from three locations within the corresponding parcel, the overall number of samples remains limited. Moreover, since the samples were taken from only three points within each parcel, this may be insufficient to fully capture the spatial variability of soil properties, potentially leading to an incomplete representation of each parcel.

The secondary limitation concerns the analysis of soil moisture content that may be affected by evaporation prior to measurement during the travel of the samples or during measurement, leading to possible underestimation of water content. These factors should be considered when interpreting the results, as they may contribute to deviations between measured and actual soil properties.

In addition, nitrogen content was not measured in this study, which represents a limitation given its central role in soil fertility and tree growth. Total nitrogen, along with the carbon-to-nitrogen ratio, would have provided valuable insight into the organic matter decomposition dynamics and nutrient cycling across the studied sites. Future analyses should aim to include nitrogen measurements to allow a more comprehensive assessment of soil quality in the context of biomass growth optimization. Beyond total nitrogen, which does not directly reflect plant-available nitrogen, measuring specific nitrogen species would also provide more meaningful insight into soil fertility. In particular, nitrate (NO_3^-) and ammonium (NH_4^+) concentrations indicate the immediately available nitrogen pool for plant uptake [32], while the carbon-to-nitrogen (C:N) ratio reflects the balance between organic matter decomposition and nitrogen mineralisation [33]. Including these complementary indicators in future analyses would allow a more nuanced understanding of nitrogen dynamics and their role in driving the observed differences in tree growth across parcels.

5.3 Conclusion

This study highlights soil pH as the central integrating indicator of soil fertility across the studied parcels in the Kérouané region of Guinea. Rather than nutrient quantity alone, it is nutrient availability, governed primarily by pH, that appears to drive the observed differences in tree growth performance between high-productivity and low-productivity parcels. Strongly acidic conditions lock up phosphorus through fixation by iron and aluminium oxides, accelerate the leaching of base cations such as calcium and magnesium, and may promote the accumulation of potentially toxic concentrations of soluble iron and manganese. These mechanisms converge to create a chemical environment unfavorable to tree establishment, even where total nutrient concentrations appear sufficient. Soil texture, through its influence on cation exchange capacity and water retention, provides a complementary physical dimension that reinforces the chemical fertility gradient identified between the two groups. Together, these findings suggest that targeted pH correction through liming or locally available amendments, combined with systematic pH assessment during site selection, could substantially improve reforestation outcomes for the arboRise Foundation. Future work should extend the sample size, incorporate nitrogen measurements, and investigate the bioavailable fraction of key nutrients in order to refine the predictive indicators of tree growth potential in this region. Beyond physicochemical parameters, this study was limited to abiotic soil properties and did not assess biological indicators such as microbial community composition, fungal networks, or soil fauna including earthworms and other invertebrates. These biological components play a fundamental role in organic matter decomposition, nutrient cycling, and soil structure formation, and their inclusion in future studies would provide a more complete understanding of the factors governing soil quality and tree growth in these reforestation contexts.

Yet reforestation alone cannot reverse the crisis. Even maximum feasible reforestation and afforestation efforts over the next 50 years would only reduce atmospheric CO concentration by 15 to 30 ppm by end of century [34], falling far short of the pre-industrial levels of 260–270 ppm [35] and representing only 3.5–7.5% of today’s concentration of 425.7 ppm [36]. Reforestation must therefore be combined with substantial reductions in greenhouse gas emissions.

References

- [1] National Centre for Climate Services. Forest functions and climate change. URL <https://www.nccs.admin.ch/nccs/en/home/the-nccs/priority-themes/forest-functions-and-climate-change.html>.
- [2] Chiara Perelli Clara Cicatiello Giacomo Branca Silvio Franco Fatoumata Binta Sombily Diallo Emanuele Blasi Giuseppe Scarascia Mugnozza Paolo Ceci, Lavinia Monforte. Small-holder farmers’ perception of climate change and drivers of adaptation in agriculture: A case study in guinea. *Review of development*, 2021. URL <https://doi.org/10.1111/rode.12815>.
- [3] FAO. Santé des sols biologique et chimique, 2024. URL <https://www.fao.org/soils-portal/soil-degradation-restoration/indicateurs-et-evaluation-de-la-sante-des-sols-du-monde/sante-des-sols-biologique-et-chimique/fr/>.
- [4] R. A. Cyamweshi, S. Kuyah, A. Mukuralinda, J. Ngango, S. R. Mbaraka, and J. D. Manirere. Farming with trees for soil fertility, moisture retention and crop productivity improvement: Perceptions from farmers in rwanda. *Small-scale Forestry*, 2023. URL <https://link.springer.com/article/10.1007/s11842-023-09547-x>.
- [5] Patrick Dugue and Christine Rawski. Gestion de la fertilité des sols en afrique subsaharienne: Recueil d’articles publiés de 1998 à 2024, 2024. URL <https://agritrop.cirad.fr/608335/1/Fascicule%20complet%20couv%20et%20sommaire.pdf>.
- [6] Arborise foundation online site. URL <https://arborise.ch/who-we-are/?lang=en>.
- [7] International Union for Conservation of Nature. Ecosystem profile: Guinean forests of west africa biodiversity hotspot, 2015. URL <https://d2910tur8o1lgj.cloudfront.net/sites/default/files/CEPF-DC28-8.pdf>.
- [8] A. Bationo, F. Lompo, and S. Koala. Research on nutrient flows and balances in West Africa: state-of-the-art. *Agriculture, Ecosystems & Environment*, 71:19–35, 1998. doi: 10.1016/S0167-8809(98)00129-7. URL <https://www.sciencedirect.com/science/article/abs/pii/S0167880998001297>.
- [9] Getachew Agegnehu, Tilahun Amede, Teklu Erkossa, Chilot Yirga, Carla Henry, Robert Tyler, Myles G. Nosworthy, Sentayehu Beyene, and Gudeta W. Sileshi. Extent and management of acid soils for sustainable crop production system in the tropical agroecosystems: a review. *Acta Agriculturae Scandinavica, Section B — Soil & Plant Science*, 71(9):852–869, 2021. doi: 10.1080/09064710.2021.1954239. URL <https://www.tandfonline.com/doi/full/10.1080/09064710.2021.1954239>.
- [10] H.Y. Ch’ng, O.H. Ahmed, and N.M.A. Majid. Improving phosphorus availability in an acid soil using organic amendments produced from agroindustrial wastes. *The Scientific World Journal*, 2014. doi: 10.1155/2014/506356. URL <https://www.hindawi.com/journals/tswj/2014/506356/>.
- [11] N. Chacon, W.L. Silver, E.A. Dubinsky, and D.F. Bhatt. Iron reduction and soil phosphorus solubilization in humid tropical forests soils. *Biogeochemistry*, 78:33–49, 2006. doi: 10.1007/

- s10533-005-2343-3. URL https://www.researchgate.net/publication/226217968_Iron_Reduction_and_Soil_Phosphorus_Solubilization_in_Humid_Tropical_Forests_Soils_The_Roles_of_Labile_Carbon_Pools_and_an_Electron_Shuttle_Compound.
- [12] Fred Adams. Crop response to lime in the southern united states. In Fred Adams, editor, *Soil Acidity and Liming*, volume 12 of *Agronomy Monographs*, pages 211–265. American Society of Agronomy, Madison, Wisconsin, 2 edition, 1984. doi: 10.2134/agronmonogr12.2ed.c5. URL <https://access.onlinelibrary.wiley.com/doi/abs/10.2134/agronmonogr12.2ed.c5>.
- [13] M.C. Sirois, H.A. Margolis, and C. Camiré. Influence of remnant trees on nutrients and fallow biomass in slash and burn agroecosystems in Guinea. *Agroforestry Systems*, 40:227–246, 1998. doi: 10.1023/A:1006093329468.
- [14] FAO. Changes in shifting cultivation in Africa, 1987. URL <https://www.fao.org/4/R5265E/r5265e06.htm>. Unasylva, Vol. 39, No. 150.
- [15] X. Wang et al. Progress in research on the effects of environmental factors on natural forest regeneration. *Frontiers in Forests and Global Change*, 2025. doi: 10.3389/ffgc.2025.1525461. URL <https://www.frontiersin.org/journals/forests-and-global-change/articles/10.3389/ffgc.2025.1525461/full>.
- [16] European Environment Agency (EEA). Characteristics of forest soils. URL <https://forest.eea.europa.eu/sandbox/forest-soils/characteristics-of-forest-soils>. Forest Information System for Europe (FISE).
- [17] Jarrod O. Miller. Soil ph affects nutrient availability, 2016. URL https://www.researchgate.net/publication/305775103_Soil_pH_Affects_Nutrient_Availability.
- [18] Dora Neina. The role of soil ph in plant nutrition and soil remediation, 2019. URL <https://onlinelibrary.wiley.com/doi/full/10.1155/2019/5794869>.
- [19] FAO. Chemical properties, 2024. URL <https://www.fao.org/soils-portal/data-hub/soil-classification/numerical-systems/chemical-properties/en/>.
- [20] Springer Nature. Role of nutrients in plant growth and development, 2020. URL https://link.springer.com/chapter/10.1007/978-3-030-41552-5_2.
- [21] Paula Ragel, Natalia Raddatz, Eduardo O. Leidi, Francisco J. Quintero, and José M. Pardo. Regulation of k⁺ nutrition in plants. *Frontiers in Plant Science*, 10:281, 2019. doi: 10.3389/fpls.2019.00281. URL <https://doi.org/10.3389/fpls.2019.00281>.
- [22] Ibrahima Saborowski Joachim Gravenhorst Gode Djomo, Adrien N. Adamou. Allometric equations for biomass estimations in cameroon and pan moist tropical equations including biomass data from africa. *Elsevier*, 260:1880, 2010. URL [https://uni-goettingen.de/de/document/download/4df40c701547ab5773871feade802dc2.pdf/Djomo_et_al_\(2010\)_FORECOLMANAG_allometric_equations.pdf](https://uni-goettingen.de/de/document/download/4df40c701547ab5773871feade802dc2.pdf/Djomo_et_al_(2010)_FORECOLMANAG_allometric_equations.pdf).
- [23] Temitope D. Timothy Oyedotun. X-ray fluorescence (xrf) in the investigation of the composition of earth materials: a review and an overview. *Geology, ecology and landscapes*, 2017. URL <https://www.tandfonline.com/doi/full/10.1080/24749508.2018.1452459#d1e194>.
- [24] Latifah Omar Prisca Divra Johan, Osumanu Haruna Ahmed and Nur Aainaa Hasbullah. Phosphorus transformation in soils following co-application of charcoal and wood ash. *Agronomy*, 11(10):2010, 2021. URL <https://www.mdpi.com/2073-4395/11/10/2010>.

- [25] Swiss Confederation. Ordinance on the remediation of contaminated sites (OSites/CSO), RS 814.680, annex 1, 1998. URL https://www.fedlex.admin.ch/eli/cc/1998/2261_2261_2261/en. As amended. Federal Office for the Environment (FOEN), Bern, Switzerland.
- [26] Cornell University Nutrient Management Spear Program.
- [27] Kathryn C. Haering and Gregory K. Evanylo. Soil and soil water relationships, 2018. URL <https://www.pubs.ext.vt.edu/BSE/BSE-194/BSE-194.html>. Publication BSE-194.
- [28] Seble Getaneh and Wubayehu Kidanemariam. Soil acidity and its managements: A review. *International Journal of Advanced Research in Biological Sciences*, 8(3):70–79, 2021. doi: 10.22192/ijarbs.2021.08.03.008. URL <https://ijarbs.com/pdfcopy/2021/mar2021/ijarbs8.pdf>.
- [29] Jianlong Wang and Shizong Wang. Preparation, modification and environmental application of biochar: A review. *Journal of Cleaner Production*, 227:1002–1022, August 2019. doi: 10.1016/j.jclepro.2019.04.282.
- [30] Lingyi Qian et al. The key role of biochar in amending acidic soil: reducing soil acidity and improving soil acid buffering capacity. *Biochar*, 2025. doi: 10.1007/s42773-025-00432-8. URL <https://link.springer.com/article/10.1007/s42773-025-00432-8>.
- [31] Mississippi State University Extension. Effects of liming materials on soil pH, 2023. URL <https://extension.msstate.edu/newsletters/forage-news/2023/effects-liming-materials-soil-ph>.
- [32] Takushi Hachiya and Hitoshi Sakakibara. Interactions between nitrate and ammonium in their uptake, allocation, assimilation, and signaling in plants. *Journal of Experimental Botany*, 68(10):2501–2512, 2017. doi: 10.1093/jxb/erw449. URL <https://academic.oup.com/jxb/article/68/10/2501/2731728>.
- [33] Daniel Geisseler et al. Nitrogen mineralization from organic fertilizers and composts: Literature survey and model fitting. *Journal of Environmental Quality*, 2021. doi: 10.1002/jeq2.20295. URL <https://acess.onlinelibrary.wiley.com/doi/10.1002/jeq2.20295>.
- [34] CORINNE LE QUÉRÉ JOANNA I. HOUSE, I. COLIN PRENTICE. Maximum impacts of future reforestation or deforestation on atmospheric co2. *Global Change Biology*, 2002. URL <https://onlinelibrary.wiley.com/doi/full/10.1111/rode.12815>.
- [35] Springer Nature. The pre-industrial carbon dioxide level, 1983. URL <https://link.springer.com/article/10.1007/BF02423528>.
- [36] Matthew W. Jones et al. Pierre Friedlingstein, Michael O’Sullivan. Global carbon budget 2025. *Earth System Science Data*, 2025. URL <https://essd.copernicus.org/preprints/essd-2025-659/>.